NATURAL CONVECTION IN A WAVY POROUS ENCLOSURE HEATED BY AN INTERNAL CIRCULAR CYLINDER

Dr. Muneer A Ismael

Mechanical Engineering Department-Engineering College – University of Basra
Email: muneerismael@yahoo.com
P.O. Box 2067, Ashar Post Office, Basra, Iraq

ABSTRACT:

Natural convection fluid flow and heat transfer of fluid-saturated porous media heated by an internal circular cylinder inside a wavy enclosure is investigated numerically. The 2D enclosure is composed of two isothermal vertical wavy walls and two adiabatic horizontal flat walls. Darcy assumption and Boussinesq approximation were relied on in this steady, incompressible study. The governing equations were solved using Galerkin finite element method implemented in FlexPDE software package. The performance of enclosure was evaluated by three non-dimensional parameters namely, the Darcy-modified Rayleigh number Ra_m (100-1000), the waviness ratio λ (0-0.35), and the position of the inner heated cylinder ξ (0.45-1.05). The results were presented by visualization of the streamline and isothermal contours and by the local and average Nusselt numbers. It was found that the lower the position of the inner cylinder (ξ=0.45) is the largest the values of Nusselt number while the influence of the wall waviness ratio is found to be very small.

KEYWORDS: Natural convection, porous media, enclosure, wavy wall, Darcy assumption.

الحمل الحر داخل وعاء مسامي متموج مسخن من الداخل باسطوانه دائريه

د.منير عبد الجليل إسماعيل

جامعه البصرة- كليه الهندسه- قسم الهندسه الميكانيكيه.

الخلاصه:

تم في هذا البحث دراسة عددية لجريان و انتقال الحرارة بالحمل الحر لمائع مشبع في وسط مسامي داخل وعاء متموج مسخن من الداخل بواسطة اسطوانة دائرية. يتكون هذا الوعاء المتموج مـن جـدارين عموديين متموجين مثبتين عند درجة حرارة ثابتة و جدارين افقيين مــستويين معــزولين حراريــا. بَنيـت التحلــيلات علــى فرضــية دارســي (Darcy assumption) وتقريبــات باوســنك (Boussinesq approximation). تم حل المعادلات الحاكمة باستخدام طريقة العناصر المحددة المزودة في حقيبة برمجية (FlexPDE). استخدمت ثلاثة معايير لا بعدية من اجل دراسة الاداء الحراري للوعاء المتموج هي: رقـم دارســـــــــــــــــــــــــــــــــي- رايلـــــــــــــــــــــــــــــــــــي المعـــــــــــــــــــــــــــــــــــــــدل Ra_m (100-1000)   نسبة التموج (0-0.35)λ و موقع الاسطوانة الداخلية المسخنة (0.45-1.05)ξ . لقد مَثلت النتائج بواسطة معاينة خطوط الجريان (streamlines) و خطوط التحارر (isotherms) وكذلك عن

طريق رقم نسلت الموقعي و المتوسط. لقد بينت النتائج بان الموقع الادنى للاسطوانة الداخليــة (0.45=ﻉ)
يعطي اكبر قيم لرقم نسلت في حين وجد ان تاثير نسبة التموج قليل جدا.

NOMENCLATURES

a	Wavy wall amplitude (m)	X,Y	Dimensionless coordinates
A	Aspect ratio	*Greek*	
D	Diameter of inner cylinder (m)	α	Thermal diffusivity of fluid (m^2/s)
Da	Darcy number	β	Thermal expansion of fluid (K^{-1})
g	Gravitational acceleration (m/s^2)	λ	Waviness ratio
h	Heat transfer coefficient (W/m^2K)	ν	Kinematic viscosity (m^2/s)
H	Enclosure height (m)	μ	dynamic viscosity of fluid (N/m^2S)
K	Permeability of porous media (m^2)	ψ	Stream function (m^2/s)
k	Thermal conductivity (W/m.K)	Ψ	Dimensionless stream function
L	Length (m)	ρ	Density of fluid (kg/m^3)
Nu	Nusselt number	ρ_o	Density of fluid at temperature To (kg/m^3)
P	Pressure (Pa)	θ	Dimensionless temperature
Ra_m	Darcy-modified Rayleigh number	ξ	Dimensionless position of inner cylinder
S	Distance along L (m)	*Subscripts*	
T	Temperature (K)	av	Average
U	Velocity vector (m/s)	c	Cold
U	Velocity in x-direction (m/s)	h	Hot
V	Velocity in y-direction (m/s)	i	Inner
W	Average width of enclosure (m)	L	Left
x,y	2D Coordinates	R	Right

1. INTRODUCTION

Fluid flow and heat transfer in porous media have received a pronounced attention in the past few decades. The reason behind this attention is the extensive growing applications of this field in engineering such as solar collectors, thermal insulation, grain storage, filtering and draying process, nuclear research (**Ingham et al 2002; Nield and Bejan 2006**), production of oil and gas from underground reservoir (**Clifford et al 2006**). The applications extend also to the biological and medical problems (**Kulasiri and Verwoerd 2003; Khaled and Vafai 2003**). Most of these applications are simulated by a natural convection process in porous enclosures. Different shaped enclosures were investigated to attain a system of high efficient thermal performance. The early reported studies, generally, were focused on the square or rectangular enclosures as in (**Groos et al 1986; Manole and Lage 1992; Goyoeau et al 1996; Baytas and Pop 2002**). Nevertheless the rectangular geometry is still investigating but in different boundary conditions as in (**Barletta and Lazzari 2005**) where a square cavity of isothermal walls and an internal concentric circular heating boundary was studied for different cavity inclination angles. The study of (**Oztop 2007**) concluded that the inclination of a partially cooled rectangular enclosure is the dominated parameter on heat transfer and fluid flow. Voral et al 2008 studied the effect of amplitude of the sinusoidaly varying temperature profile on the bottom wall of rectangular enclosure for different aspect ratios. Another study on square enclosure subjected to localized heating and salting from one side was done by (**Zaho 2008**) where the double-diffusive convective flow was considered (double-diffusive: diffusion of matter caused by temperature gradients and diffusion of heat caused by concentration gradient). In (**Braga and Lemos 2009**) a numerical tool was developed to study the natural convection in a composite cavity formed by three distinct regions, clear, porous, and solid region.

However, a limited group of non-rectangular porous enclosures was investigated basing on Darcian and non-Darcian assumptions of porous model. The trapezoidal enclosure has been studied by many researchers; in (**Marafi and Vafai 2001**) a numerical parallel analysis was developed to study the effect of Darcy modified Rayleigh number Ra_m, Grashof number, and the inclination of the trapezoidal walls. Extensive numerical studies, penalty finite element with bi-quadratic element analysis was performed to study the wall inclination, uniform and non uniform heating of the trapezoidal base and wide range of Rayleigh, Prandtle and Darcy parameters are edited in (**Basak et al 2009**) and in another work (**Basak et al 2009**). A right angle trapezoidal enclosure with heated vertical wall and partially cooled inclined wall was studied by (**Voral et al 2009**). Three aspect ratios and three locations of cooling part with a range of Ra_m were examined. In addition, the maximum density effect on buoyancy-induced flow and heat transfer was studied in (**Voral et al 2010**). Right-angle triangular enclosures were studied numerically for various boundary conditions of the walls, various aspect ratios and ranges of Ra_m (**Voral et al 2006**). In addition, the effect of adding a thin fin inside the right-angle triangular enclosure was investigated in (**Voral et al 2007**). The effect of inserting a square body subjected to four different boundary conditions inside the right-angle triangular enclosure was investigated in (**Voral et al 2007**).

Because of its complexity, fewer published works about wavy wall(s) enclosures filled with porous media were found. The studies reported in (**Mahmud and Andrew 2004, Adjlout et al 2002, Mahmud et al 2002, Mahmud et al 2003**) deal with wavy wall enclosures but limited to clear fluid only. The works of (**Kumar and Shalini 2003, Misirlioglu et al 2005, Khanafer et al 2009, Sultana and Hyder 2007**) are concerned with wavy wall(s) porous enclosures based on non-Darcian assumption. In all these studies, besides to the classical parameters, Ra, Gr, etc., the effect of phase wavelength and amplitude of the wavy wall(s) were examined.

A wavy porous enclosure heated by an internal body has not been seen previously investigated. Therefore, the present study try to contribute in this field of investigation by studying the natural convection in a wavy wall enclosure filled with fluid-saturated porous medium heated by inside circular cylinder basing on Darcian assumption.

2. MATHEMATICAL MODELING
2.1 Physical model

Generally, the low velocity flow which is the case in porous media flow obeys Darcy's law (Clifford et al 2006),

$$\frac{\mu}{K}U = -\nabla P + \rho\boldsymbol{g} \tag{1}$$

Where μ and ρ are the dynamic viscosity and the density of the fluid respectively, K is the permeability of the porous media, P is the pressure, U=(U,V) is the velocity vector and $\boldsymbol{g}$=(0,-g) is the gravitational acceleration. The effects of inertia and boundary permeability are ignored in this study i.e. basing the modeling according to Darcy assumption which is can be safely applied when Darcy number Da $< 10^{-4}$ (Clifford 2006). The properties of fluid are considered constant everywhere except the density in the buoyancy term of momentum equation which is Boussineq approximation according to the following linear equation of state:

$$\rho = \rho_o\left[1 - \beta\left(T - T_o\right)\right] \tag{2}$$

Hence the equations governed the problem are: continuity, Darcy-momentum, and energy equations. The Darcy momentum is obtained by differentiating the x-component of equ.(1) with respect to y and that of y- component with respect to x and subtracting the resulting two equations. The following dimensional set of equations is obtained.

$$\frac{\partial U}{\partial x} + \frac{\partial V}{\partial y} = 0 \tag{3}$$

$$\frac{\partial U}{\partial y} - \frac{\partial V}{\partial x} = -\frac{g\beta K}{\nu}\frac{\partial T}{\partial x} \tag{4}$$

$$U\frac{\partial T}{\partial x} + V\frac{\partial T}{\partial y} = \alpha\left(\frac{\partial^2 T}{\partial x^2} + \frac{\partial^2 T}{\partial y^2}\right) \tag{5}$$

Using the stream function ψ definition; $U = \dfrac{\partial \psi}{\partial y}$, $V = -\dfrac{\partial \psi}{\partial x}$ and scaling the different variables as follow: $X = \dfrac{x}{W}$, $Y = \dfrac{y}{W}$, $\Psi = \dfrac{\psi}{\alpha}$, $\theta = \dfrac{T - T_c}{T_h - T_c}$ where W is the average width of the enclosure shown in **Figure** 1. Thus, the governing equs.(3-5) can be written in the following non-dimensional form:

$$\frac{\partial^2 \Psi}{\partial X^2} + \frac{\partial^2 \Psi}{\partial Y^2} = -Ra_m\frac{\partial \theta}{\partial X} \tag{6}$$

$$\frac{\partial \Psi}{\partial Y}\frac{\partial \theta}{\partial X} - \frac{\partial \Psi}{\partial X}\frac{\partial \theta}{\partial Y} = \frac{\partial^2 \theta}{\partial X^2} + \frac{\partial^2 \theta}{\partial Y^2} \tag{7}$$

Where Ra_m is the Darcy modified Rayleigh number:

$$Ra_m = Ra.Da = \frac{g\beta(T_h - T_c)W^3}{\nu\alpha}\frac{K}{W^2} = \frac{g\beta K(T_h - T_c)W}{\nu\alpha}$$

The local Nusselt numbers for both wavy surfaces and the inside circular surface are calculated from:

$$Nu_L = \frac{h_L L_L}{k}, \; Nu_R = \frac{h_R L_R}{k}, \; Nu_i = \frac{h_i L_i}{k} \tag{8}$$

Where h is the local heat transfer coefficient given by:

$$h = -\frac{k}{\Delta T}\frac{\partial T}{\partial \mathsf{n}} \tag{9}$$

k is the thermal conductivity, L_L and L_R are the left and right wavy lengths respectively, Li is the inner cylinder perimeter$=\pi$D and **n** is a vector normal to the wall. Hence, the local Nusselt numbers are as follows:

$$Nu_L = -\frac{\partial \theta}{\partial \mathsf{n}}, \; Nu_R = -\frac{\partial \theta}{\partial \mathsf{n}}, \; Nu_i = -\frac{\partial \theta}{\partial \mathsf{n}} \tag{10}$$

The average Nusselt number over the surfaces can be written as

$$Nu_{av,L} = -\frac{1}{L_L}\int_{S_L}\frac{\partial \theta}{\partial \mathsf{n}}dS_L, \; Nu_{av,R} = -\frac{1}{L_R}\int_{S_R}\frac{\partial \theta}{\partial \mathsf{n}}dS_R, \; Nu_{av,i} = -\frac{1}{\pi D}\int_{Si}\frac{\partial \theta}{\partial \mathsf{n}}dS_i \tag{11}$$

Due to symmetry about X=0, and steady-state assumption, the average Nusselt numbers along both the wavy walls and the inner cylinder are related according to the overall heat balance;

$$Nu_{av,L} \times L_L + Nu_{av,R} \times L_R = Nu_{av,i} \times \pi D \tag{12}$$

2.2 Boundary conditions

The enclosure is made of two horizontal flat walls and two vertical wavy walls with inside circular cylinder (**Figure** 1). The space between the inside cylinder and the enclosure walls is filled with fluid-saturated porous medium. The flat horizontal walls are kept adiabatic while the wavy walls and the inner cylinder are isothermal but kept at different temperatures (the temperature of inner cylinder is higher). The position of the inside cylinder can be moved along a vertical line X=0. The definitions of the boundaries and their conditions are as follow:

$i)\dfrac{\partial \theta}{\partial Y} = 0, \Psi = 0$ at Y=0 and at Y=A, with X ranges: $-\left(\dfrac{1}{2} - \lambda\right) \le X \le \left(\dfrac{1}{2} - \lambda\right)$ for both Y's

$ii)\theta = 0,\ \Psi = 0$ on the left wavy wall $0 \le Y \le A,\quad X = \left(\dfrac{1}{2} - \lambda\right) + \lambda\left[1 - \sin\left(\dfrac{\pi}{2} + \dfrac{2\pi Y}{A}\right)\right]$ and on the

right wall $0 \le Y \le A,\quad X = -\left(\dfrac{1}{2} - \lambda\right) - \lambda\left[1 - \sin\left(\dfrac{\pi}{2} + \dfrac{2\pi Y}{A}\right)\right]$

$iii)\theta = 1,\ \Psi = 0$ on the inside circular cylinder circumference. Here λ denotes to the vertical waviness =a/W, and A is the aspect ratio = H/W =1.5= 4D, W is the average width of the enclosure.

3. NUMERICAL SOLUTION AND VALIDATION
3.1 Software overview

The non-dimensional equations system (equs.6-7) is to be solved numerically by mean of the software package FlexPDE Professional Version 5.0.20 3D. The FlexPDE is a scripted finite element model builder and numerical solver written by user (**Gunnar 2005**). It performs the operations necessary to turn a description of a partial differential equations system into a finite element model, solve the system, and present graphical and tabular output of the results. It has no pre-defined problem domain or equation list, i.e. the domain geometry and the partial differential equations are totally achieved by the user. The FlexPDE is combined of several modules to provide a complete problem solving system, these are:

- **A script editing module** with syntax highlighting provides a full text editing facility and a graphical domain preview.
- **A symbolic equation analyzer** expands defined parameters and relations, performs spatial differentiation, and symbolically applies integration by parts to reduce second order terms to create symbolic Galerkin equations. It then symbolically differentiates these equations to form the Jacobian coupling matrix.
- **A mesh generation module** constructs a triangular or tetrahedral finite element mesh over a two or three-dimensional problem domain. In two dimensions, an arbitrary domain is filled with an unstructured triangular mesh. In three-dimensional problems, an arbitrary two-dimensional domain is extruded into the third dimension and cut by arbitrary dividing surfaces. The resulting three-dimensional figure is filled with an unstructured tetrahedral mesh
- **A Finite Element numerical analysis module** selects an appropriate solution scheme for steady-state, time-dependent or eigenvalue problems, with separate procedures for linear and nonlinear systems. The finite element basis may be either quadratic or cubic.
- **An adaptive mesh refinement procedure** measures the adequacy of the mesh and refines the mesh wherever the error is large. The system iterates the mesh refinement and solution until a user-defined error tolerance is achieved.

- **A dynamic time step control procedure** measures the curvature of the solution in time and adapts the time integration step to maintain accuracy.
- **A graphical output module** accepts arbitrary algebraic functions of the solution and plots contour, surface, vector or elevation plots.
- **A data export module** can write text reports in many formats, including simple tables, full finite element mesh data, CDF or TecPlot compatible files.

An example of customized graphical outputs is shown in **Figure 2** and the edited script of the present work is presented in **appendix 1**. The results are to be represented by stream lines, isotherms and local and average Nusselt numbers. The contours plots are directly captured from the output screen but the data of Nusselt number were exported to another Grapher tool to be able of showing more than one curve in single plot.

3.2 Software validation

To check the validity of the present used software, and enhance the reliability of the obtained results, the average Nusselt number along the perimeter of the inner cylinder $Nu_{av,i}$ was evaluated at five grid densities and for three values of Darcy modified Rayleigh number Ra_m. The grid density in this package is controlled by imposing a relative error together with a mesh refinement times. The relative error was varied from 10^{-2} to 10^{-6} and the mesh refinement times were left to be free. The results are presented in **Figure 3**. It can be seen that at low Ra_m, the results are slightly affected by the grid size. But at higher Ra_m ($Ra_m > 500$), there is a noticeable sensitivity of the results to the grid size especially at $Ra_m = 700$. However, this figure indicates that when the relative error $\leq 10^{-4}$ i.e. higher grid density, the results of $Nu_{av,i}$ are approximately fixed for all Ra_m's. Accordingly, a relative error of 10^{-4} was chosen in this study as a compromise between the accuracy of the results and the time consumed in each run. Some cases take a run time of about 900 seconds. The girded domain of 10^{-4} relative error is shown in **Figure** 4 which indicates that FlexPDE is adaptively refining the mesh wherever it detects that there are strong curvature in the solution domain.

4. RESULTS AND DISCUSSION

To enhance the validation of the present numerical results, a comparison with other works was conducted for two different physical domains. These two domains have flat walls ($\lambda=0$) with ($A=1$) i.e. square enclosure, and filled with fluid-saturated porous media according to Darcian assumption. The first case is that of (**Barletta and Lazzari 2005**) where there exist an internal concentric circular cylinder subjected to a uniform heat flux while the flat walls are kept isothermal at $\theta=0$. The results are presented in **Table**1 by average Nusselt number on the internal circumference. The second case which was investigated in more than one published works is free of any internal body and adiabatic horizontal walls and isothermal (but with different temperature) vertical walls (**Misirlioglu et al 2005**). The results are presented in **Table**2 by average Nusselt number on the isothermal walls. It seen that there is a very good agreement between the present results of $Nu_{av,i}$ and the two different cases. Therefore, the confidence in using the present numerical package is highly enhanced.

The effects of Darcy modified Rayleigh number Ra_m, wall waviness ratio (λ) and the position of the inner cylinder ($\xi=Y/A$) were investigated by the aids of visualization of streamlines, isotherms, and local and average Nusselt numbers. The examined ranges of Ra_m is from 100 to 1000; λ: 0, 0.1, 0.25, 0.35; and ξ: 0.45, 0.55, 0.75 (enclosure center), 0.95, and 1.05. The results are figured and gathered in the following two categories.

4.1 Stream and isothermal lines

Figure 5 shows the streamlines inside the enclosure of $\lambda=0.1$ and $Ra_m=100$ (upper row) and $Ra_m=1000$ (lower row) for three different values of ξ (1.05, 0.75 and 0.45). In all these cases, a double symmetric circulation cells with different directions is noticed. The clockwise direction is denoted by negative sign of stream function while the anticlockwise one is denoted by the positive sign. However, the double circulation cells are formed as the hot fluid moves up from the

surroundings of inner cylinder towards the adiabatic upper flat wall and turn to the neighboring wavy wall (in both sides) where it mixes with cold fluid stream falling down along the wavy (cold) walls. Thus, the center of these circulation cells is over the inner cylinder center in all these subfigures. The offset between the two centers increases with lowering ξ (the inner cylinder center) resulting in a more strength circulation occupying large space of enclosure as in the case of ξ=0.45 where the fluid circulation covers most of the enclosure space. When Ra_m is increased, the strength of stream function is increased also where its value at Ra_m=1000 is about five times that when Ra_m=100. This is due the domination of the convection over conduction which in turn leads to a good circulation inside the enclosure

Figure 6 shows the isotherms for the previous case (λ=0.1, Ra_m=100, 1000, ξ=1.05, 0.75, 0.45). At low Ra_m(=100), the upper row of **Figure** 6, a parallel lines are observed around the inner cylinder except at its upper portion where a plume like distribution is observed and this distribution is grow when the inner cylinder is lowered. It is seen that the temperature gradient between the inner cylinder surface and the porous media is minimum at the source regime of the plume like distribution. For higher Ra_m and especially at Ra_m=1000, as presented in the lower row of **Figure** 6, the isothermal lines take the shape of tangent function or what is called climbing sine function ($\pm$ sin x $\pm$ x). The plume like distribution at the upper portion of the inner cylinder is sharper here and its regime is limited. This complex distribution of isotherms is due to the enhanced convection. It is seen that lowering the position of the inner cylinder also enhance the convection heat transfer due to the increased contribution space of the enclosure filled with porous medium. Generally, a thermal boundary layer appears on the upper part of the wavy walls. This thermal boundary layer becomes thinner at high Ra_m as it appears from **Figure** 6.

The parameters of **Figure 7** are same as that of **Figures 5 and 6** except λ=0.35. There is no specified difference between the distribution and the magnitude of stream function except in the case of Ra_m=100 and ξ=1.05 where the center of the double circulation cells is below that of the inner cylinder. This because the geometry of the enclosure at λ=0.35, where the flat adiabatic wall length is significantly small and the upper (and lower) part of the wavy cold walls is semi-horizontal which concentrates the faller cold stream far away from the inner cylinder. On the other hand, the isotherms of **Figure 8** which are refer to the same previous case of λ=0.35 could be classified into two patterns. In the first pattern Ra_m=100 (upper row of **Figure 8**), the isotherm behavior is similar to that when λ=0.1 but the temperature is less at the upper part of the enclosure. While the isotherms of Ra_m=1000 (lower row of **Figure 8**) behaves exactly as same as that of λ=0.1.

4.2 Variations of Nusselt number

The local Nusselt number is examined along the circumference of the inner cylinder and the right wavy wall. **Figure 9** illustrates the distribution of the local Nusselt number along the circumference of the inner cylinder for three Ra_m (100, 500, 1000) and three values of ξ (1.05, 0.75, 0.45) and for λ=0.25. For all these six parameter combinations, the distribution of Nusselt number is symmetric (with one peak) about the vertical line X=0 which appears in figures at Si=0.5. The values of Nu_i increase with increasing Ra_m due to the added heat transfer which is seen clearly from the stronger circulation at high Ra_m shown in **Figures 5 and 7**. The peaks appear at Si=0.5 i.e. at the lowest point of the circumference because of the temperature gradient here is maximum as it previously clarified on the isothermal lines of **Figures 6 and 8**. It is seen also that the curvature of the two sides of the bell shaped distribution of Nu_i diminishes with lowering the inner cylinder position. It becomes completely straight line at ξ=0.45, thus resulting in an increase in the overall heat transfer (the area under curves). The virtue of this increase in heat transfer refers to that at lower values of ξ, a more space of enclosure will be subjected to the convection from the inner cylinder. Finally the peak of Nu_i distribution of the case ξ=0.45 and Ra_m=100 becomes more flat along the segment 0.25<Si<0.75. This is because the uniform temperature gradient along this segment as it appears from isotherms of **Figures 6 and 8**.

Figure 10 shows the variation of Nusselt number along the right wavy wall for the same parameters of **Figure 9**. Generally, the values of local Nusselt number increases monotonically along the wavy wall from bottom to top depending on the inner cylinder position. When the cylinder is at the upper position $\xi=1.05$, the heat may transfer across only one-half of the wavy wall as seen in **Figure 10**. More length of wavy wall contributes in heat transfer process when ξ is lowered as seen from **Figures 10 b and c**. Thus, increasing the area under curves (averaged Nusselt number) results in an improved heat transfer through the enclosure. The increase of local Nusselt number with Ra_m is attributed to the good circulation at higher Ra_m values as explained previously in the lower rows of **Figure 5 and 7**. Also at higher Ra_m, the increase of Nusselt number values becomes steeper near the upper part of the wavy walls. This is due to the high temperature gradient between the wavy wall and the fluid inside the porous enclosure as shown previously in **Figures 6 and 8**. It is convenient to mention here that the variation of local Nusselt number along the left wavy wall is not shown because it is the mirror of that of the right wavy wall.

To imagine the effect of Ra_m, ξ and λ on the overall heat transfer process, the inner cylinder circumference-averaged Nusselt number is graphed with Ra_m in **Figures 11 and 12**. **Figure** 11 shows the effect of Ra_m and ξ on the average Nusselt number for three waviness ratios. The variation of $Nu_{av,i}$ is as expected; increases with Ra_m. Heat transfer becomes larger when ξ is lowered, this effect clearly appears in **Figure** 11 a, b and **c**. For example, at $Ra_m=1000$, an increase in $Nu_{av,i}$ of about 19% is gained when ξ is lowered from 1.05 to 0.45. The lowest two positions of inner cylinder exhibit less variation than other positions. This is due to the variation of convection dominance with the inner cylinder position. The implication of an insight to **Figures 11 a, b, and c** is that there is no pronounced effect of λ.

Alternatively, **Figure 12** shows the effect of Ra_m and λ on $Nu_{av,i}$ for various values of ξ. The effect of λ on $Nu_{av,i}$ can be sensed in few situations of this study but is generally is very small. When the inner cylinder is at highest position ($\xi=1.05$), the effect of λ is maximum (**Figure 12a**). This is because that the surface of inner cylinder is closest to the wavy surface and in this portion of enclosure the concentrated stream function and temperature gradient is maximum due to convection. A waviness value of $\lambda=0.25$ exhibit more improvement of heat transfer. This scenario is enhanced in **Figure12c** where the inner cylinder is at lowest position ($\xi=0.45$). Here when $Ra_m=400$, the effect of λ is squeezed due to the dominance of convection in most of the enclosure. **Figure 12b** implies to no sensed variation of $Nu_{av,i}$ with λ. **Figures 12b and c** show an inverse effect of the waviness λ. **Figures 12a-c** can be specified from the two ends of each curve, where they have higher values of $Nu_{av,i}$ with lowering ξ.

5. CONCLUSIONS

Natural convection heat transfer and fluid flow inside a fluid-saturated porous media wavy enclosure heated by an internal circular cylinder was investigated basing on Darcian assumptions. The appliance of investigation was Galerkin finite-element method implemented through the software package (FlexPDE). The effect of three dimensionless parameters was studied namely; Darcy modified Rayleigh number, inner cylinder position, and waviness of wavy walls. The results led us to the following conclusions

i-For any values of inner cylinder position and wall waviness, the heat transfer is an increasing function of Darcy modified Rayleigh number.

ii- Higher heat transfer is obtained when the inner cylinder is positioned below the mid enclosure height and whatever the wall waviness be.

iii- Little influence of wall waviness on heat transfer when the inner cylinder is positioned above the mid-enclosure height, otherwise, there is no influence of wall waviness.

REFERENCES

Adjlout L., Imine O., Azzi A., and Belkadi M., 2002, "Laminar natural convection in an inclined cavity with a wavy wall" International Journal of Heat and Mass Transfer Vol. 45 2141–2152.

Barletta A**.**, and Lazzari S., 2005, "2D free convection in a porous cavity heated by an internal circular boundary" Excerpt from the Proceedings of the COMSOL Metaphysics User's Conference Stockholm

Basak T, Roy S., Singh A., and Pop I., 2009, "Finite element simulation of natural convection flow in a trapezoidal enclosure filled with porous medium due to uniform and non-uniform heating" International Journal of Heat and Mass Transfer Vol. 52 70–78.

Basak T, Roy S., Singh A. and Balakrishnan A.R., 2009, " Natural convection flows in porous trapezoidal enclosures with various inclination angles" International Journal of Heat and Mass Transfer Vol.52 4612–4623.

Baytas A.C. and Pop I., 1999, "Free convection in oblique enclosures filled with a porous medium" Int. J. Heat Mass Transfer Vol.42 pp1047–1057.

Baytas A.C. and Pop I. 2002,   "Free convection in a square porous cavity using a thermal non equilibrium model" Int. J. Therm. Sci. Vol. 41 861–870.

Braga E. J., Marcelo J.S. de Lemos, 2009, "Laminar and turbulent free convection in a composite enclosure" International Journal of Heat and Mass Transfer Vol. 52 588–596.

Clifford K., Ho Stephen and W. Webb, 2006 "Gas Transport in Porous Media" Springer.

Goyeau B., Songbe J.P., and Gobin D., 1996, "Numerical study of double-diffusive natural convection in a porous cavity using the Darcy-Brinkman formulation" Int. J. Heat Mass Transfer Vol.39 1363–1378.

Gross R.J., Bear M.R. and Hickox C.E., 1986, "The application of flux-corrected transport (FCT) to high Rayleigh number natural convection in a porous medium" in: Proc. 8th Int. Heat Transfer Conf., San Francisco, CA.

Gunnar B., 2005, "Fields of Physics by Finite Element Analysis Using FlexPDE" by GB Publishing and Gunnar Backstrom Malmo, Sweden

Ingham D. B. and Pop I., 2002, "Transport Phenomena in Porous Media II" first edition Elsevier Science,

Khaled A.-R.A. and Vafai K. 2003, "The role of porous media in modeling flow and heat transfer in biological tissues" International Journal of Heat and Mass Transfer Vol.46 4989–5003.

Khanafer K., Al-Azmi B. and Marafie A., Pop I., 2009, "Non-Darcian effects on natural convection heat transfer in a wavy porous enclosure" International Journal of Heat and Mass Transfer Vol.52 1887–1896.

Kulasiri D. and Verwoerd W., 2002, "Stochastic Dynamics Modeling Solute Transport in Porous Media" First edition Elsevier Science B.V.

Kumar B.V. R., and Shalini, 2003,   "Free convection in a non-Darcian wavy porous enclosure" International Journal of Engineering Science Vol.41 1827–1848.

Mahmud S, Kumar P., Hyder N. and Sadrul Islam A.K.M., 2002, "Free convection in an enclosure with vertical wavy walls" International journal of Thermal Science Vol.41 440–446.

Mahmud S., Sadrul Islam A.K.M., 2003, "Laminar free convection and entropy generation inside an inclined wavy enclosure, International Journal of Thermal Sciences Vol.42 1003–1012.

Mahmud S. Frase and R. A., 2004, "Free convection and entropy generation inside a vertical in phase wavy cavity" Int. comm., Heat Mass Transfer, vol. 31, No. 4, pp 455-466.

Manole D.M., Lage J.L. 1992, "Numerical benchmark results for natural convection in a porous medium cavity" in: Heat and Mass Transfer in Porous Media ASME Conf. HTD-216, pp. 55 -60.
Marafie A. and Vafai K., 2001, "Analysis on Non-Darcain effect on Temperature Differentials in porous media" International Journal of Heat and Mass Transfer Vol.44 4401–4411.

Misirlioglu **A**., Baytas A.C., and Pop I., 2005, "Free convection in a wavy cavity filled with a porous medium" International Journal of Heat and Mass Transfer Vol. 48 1840–1850.

Moya S.L., Ramos E., and Sen M., 1987, "Numerical study of natural convection in a tilted rectangular porous material" Int. J. Heat Mass Transfer Vol.30 pp 741–756.

Nield D.A**.** and Bejan A., 2006, "Convection in Porous Media" third edition, Springer Science + Business Media, Inc., New York..

Oztop H. F., "Natural convection in partially cooled and inclined porous rectangular Enclosures" International Journal of Thermal Sciences Vol.46 149–156 2007

Sultana Z**.**, and Hyder N., 2007, "Non-darcy free convection inside a wavy enclosure" International Communications in Heat and Mass Transfer Vol.34 136–146.

Varol Y, Oztop H, F., and Varol A., 2006, "Free convection in porous media filled right-angle triangular enclosures" International Communications in Heat and Mass Transfer Vol.33 1190–1197.

Varol Y, Oztop H. F., and Varol A, 2007, "Effects of thin fin on natural convection in porous triangular enclosures" International Journal of Thermal Sciences Vol.46 1033–1045.

Varol Y, Oztop H. F., and Yilmaz T., 2007, "Two-dimensional natural convection in a porous triangular enclosure with a square body" International Communications in Heat and Mass Transfer Vol.34 238–247.

Varol Y**,** Oztop H. F. and Pop I., 2008, "Numerical analysis of natural convection for a porous rectangular enclosure with sinusoidally varying temperature profile on the bottom wall" International Communications in Heat and Mass Transfer Vol.35 56–64.

Varol Y, Oztop H. F., and Pop I., 2009, "Natural convection in right-angle porous trapezoidal enclosure partially cooled from inclined wall," International Communications in Heat and Mass Transfer Vol. 36 6–15.

Varol Y, Oztop H. F., and Pop I., 2010, "Maximum density effects on buoyancy-driven convection in a porous trapezoidal cavity" International Communications in Heat and Mass Transfer Vol. 37 401–409.

Zhao F., Liu D., and Tang G., 2008, "Natural convection in a porous enclosure with a partial heating and salting element" International Journal of Thermal Sciences Vol.47 569 583.

Table 1 Values of averaged Nusselt number along the circumference of internal cylinder-Comparision with the case of (Barletta and Lazzari 2005)

L/D		2			4	
Ra_m	300	1000	3000	300	1000	3000
Barleta and Lazzari 2005	5.791	7.786	11.17	6.951	10.25	15.07
Present	5.791	7.785	11.165	6.952	10.246	15.065

Table 2 Values of averaged Nusselt number on the isothermal walls of square cavity-Comparision with the case of (Misirlioglu et al 2005) and other references cited in it.

Authors	$Ra_m=10$	$Ra_m=100$	$Ra_m=1000$
Misirlioglu et al 2005	1.19	3.05	13.15
Moya 1987	1.065	2.801	-
Baytas and Pop 1999	1.079	3.16	14.06
Present	1.0795	3.135	13.915
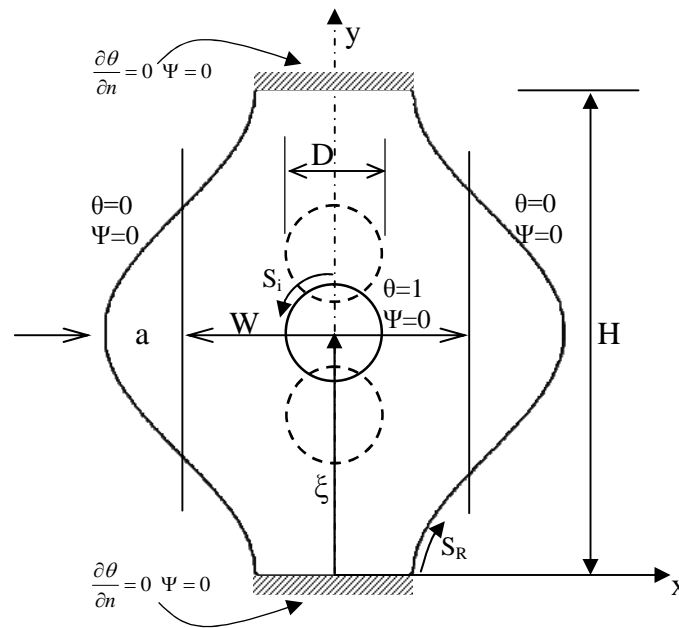
Fig.1 Physical domain of the enclosure
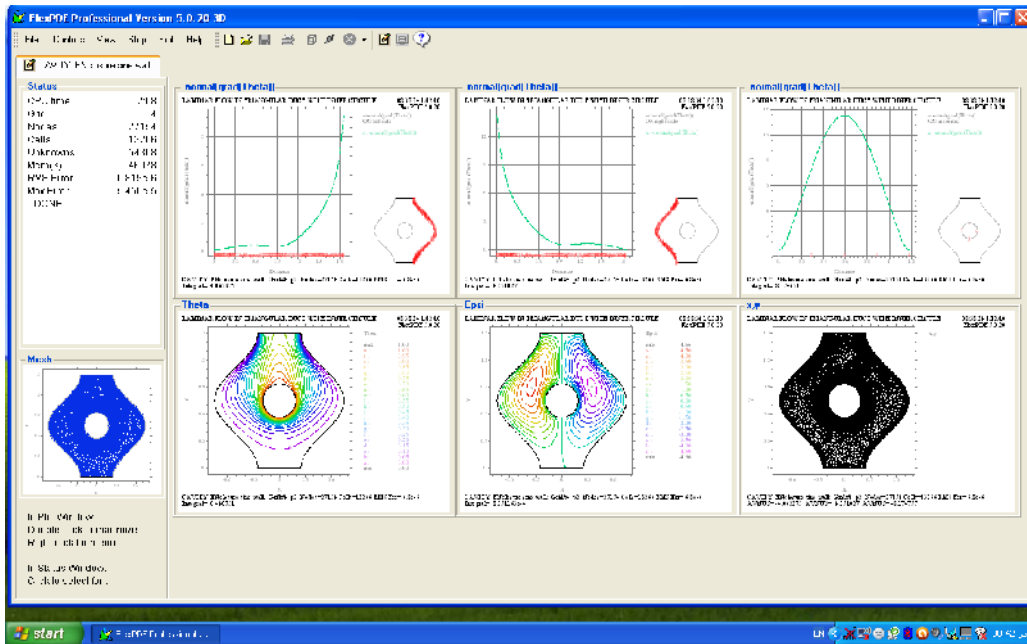
Fig.2 An example of customized graphical results
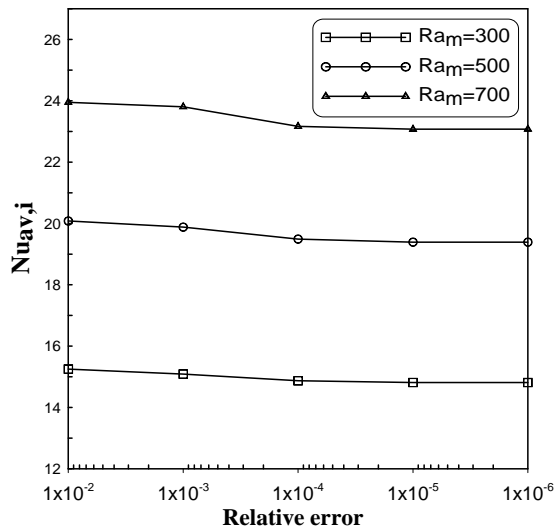
Fig.3 Variation of average Nusselt number with the relative error (number of grids)λ=0.25, ξ=0.75
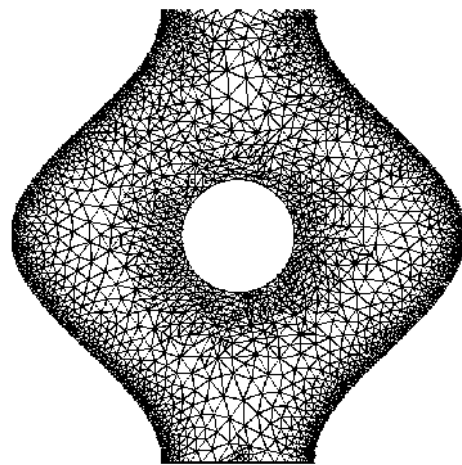
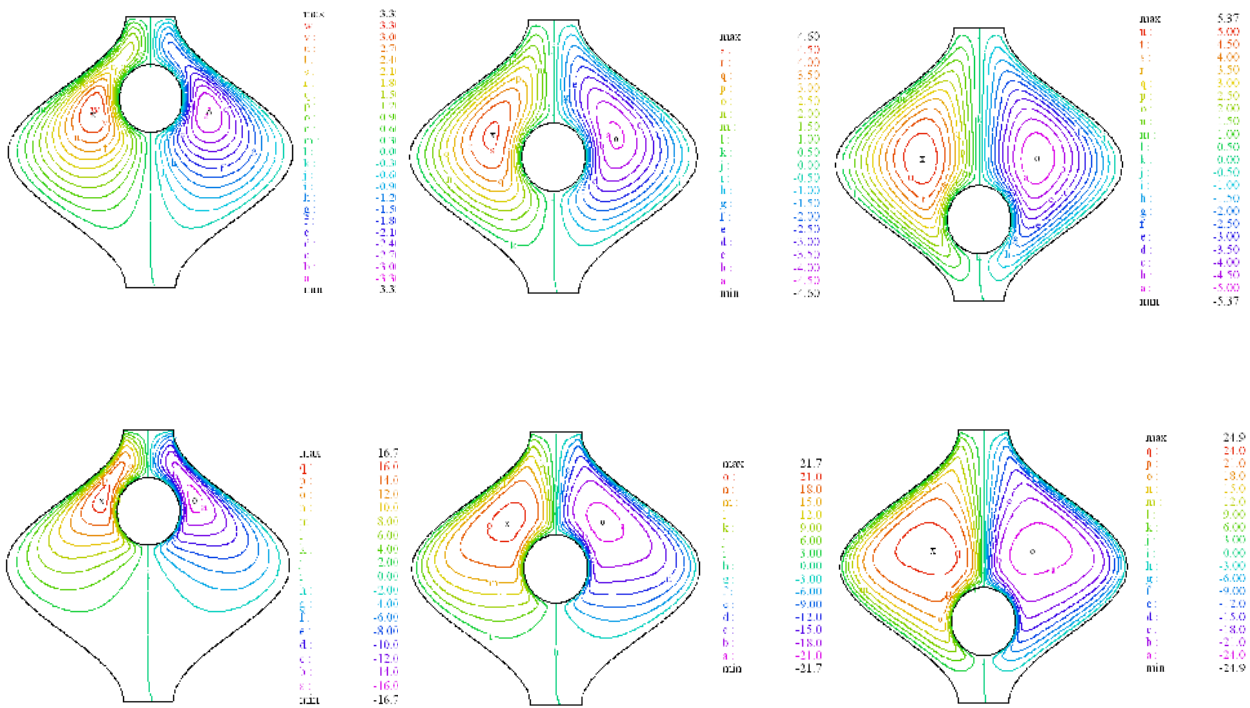Fig.4 Distribution of grids (10806 nodes) over the domain of Ra_m=100, λ=0.25, ξ=0.75
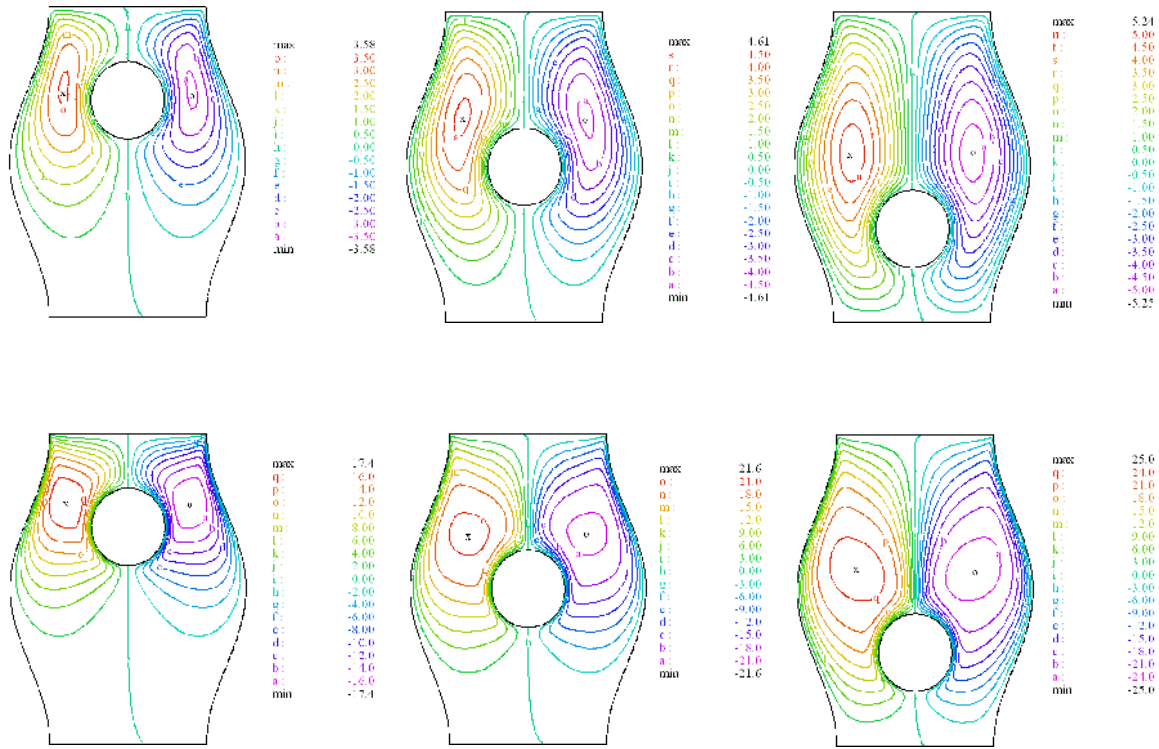
Fig.5 Streamlines for $\lambda=0.1$, and $Ra_m=100$ (upper row), 1000 (lower row), $\xi=1.05$ (left column), 0.75(middle column) and 0.45 (right column)
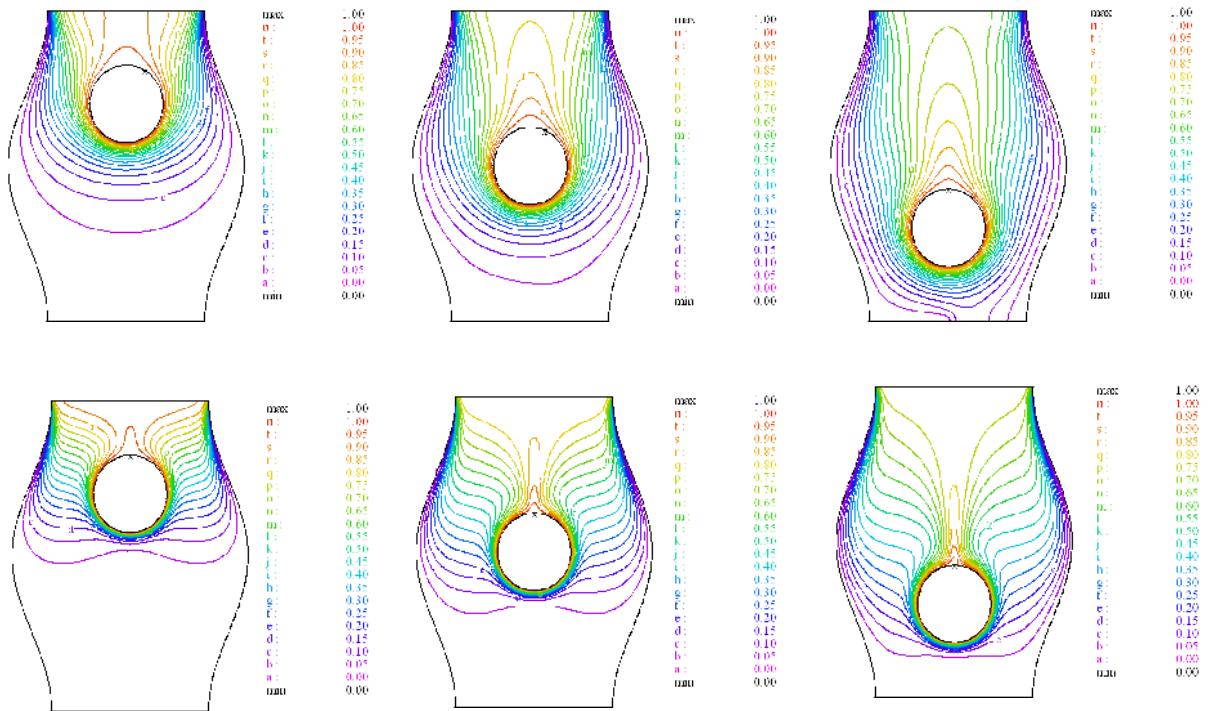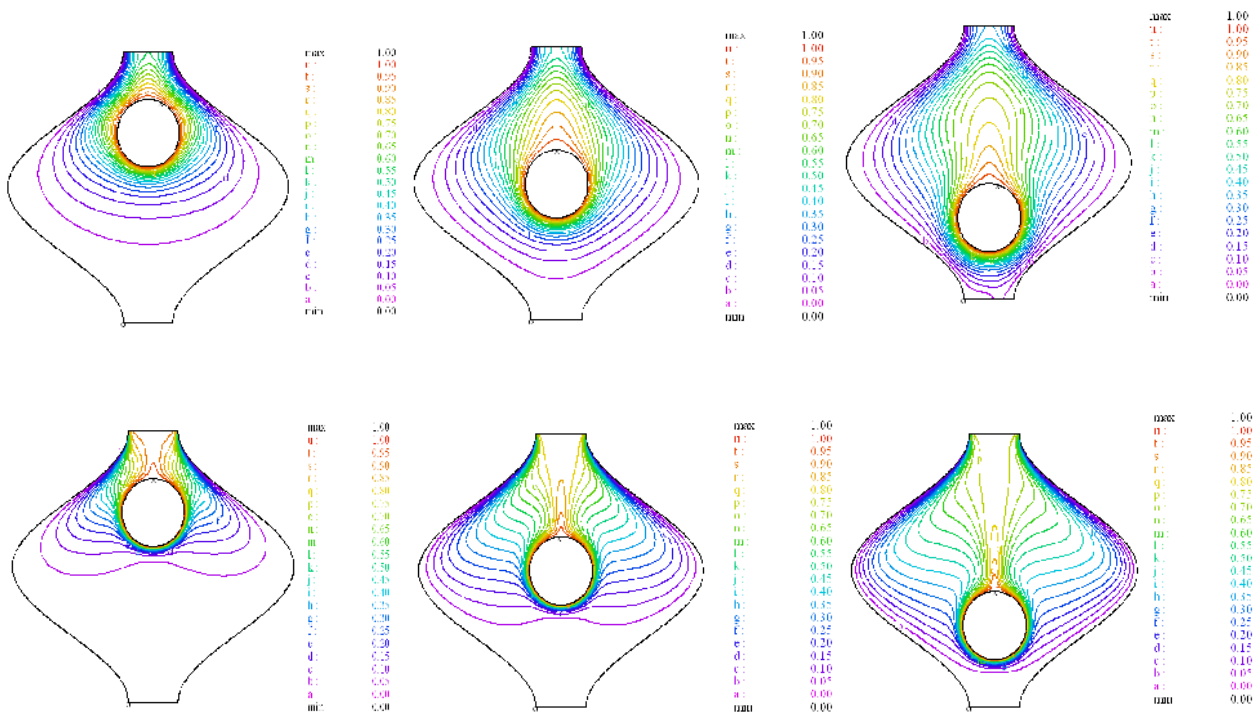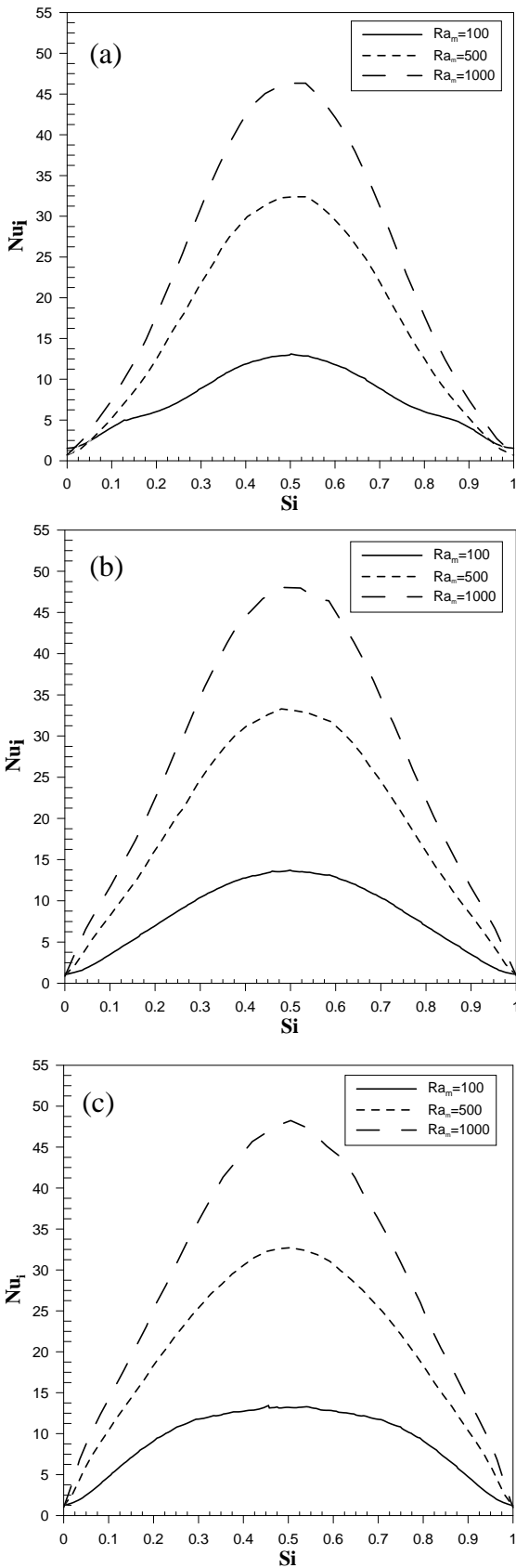

Fig.6 Isotherms for $\lambda=0.1$, and $Ra_m=100$ (upper row), 1000 (lower row), $\xi=1.05$ (left column), 0.75(middle column) and 0.45 (right column)

Fig.7 Streamlines for λ=0.35, and Ra$_m$=100 (upper row), 1000 (lower row), ξ=1.05 (left column), 0.75(middle column) and 0.45 (right column)

Fig.8 Isotherms for λ=0.35, and Ra$_m$=100 (upper row), 1000 (lower row), ξ=1.05 (left column), 0.75(middle column) and 0.45 (right column)

Fig.9 Variation of local Nusselt number along the inner cylinder cicumference for λ=0.25 and and (a)ξ=1.05, (b)ξ=0.75, (c)ξ=0.45
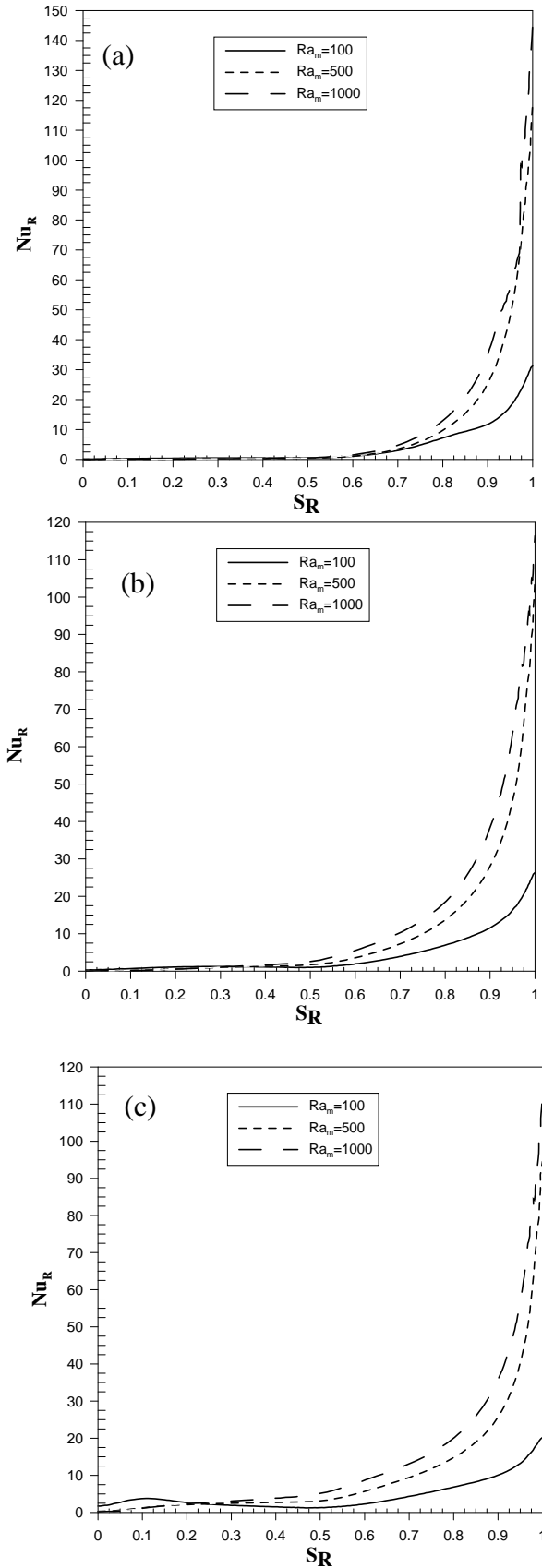
Fig.10 Variation of local Nusselt number Along the right wavy wall for λ=0.25 and (a)ξ=1.05,(b)ξ=0.75,(c) ξ=0.45
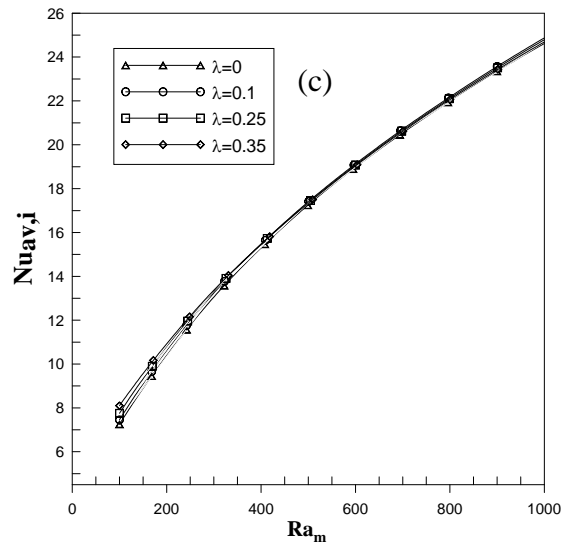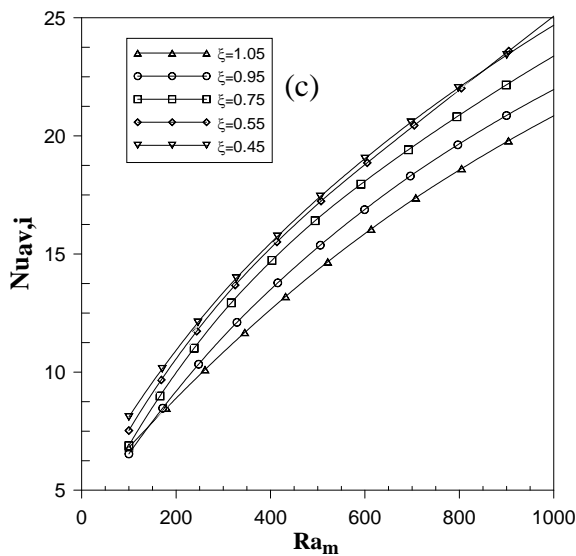
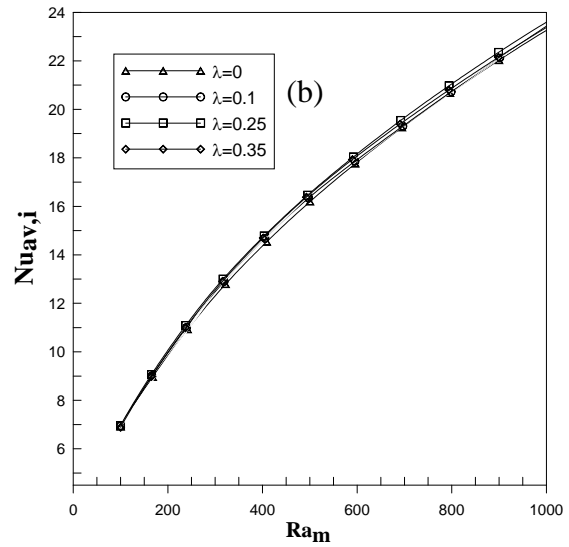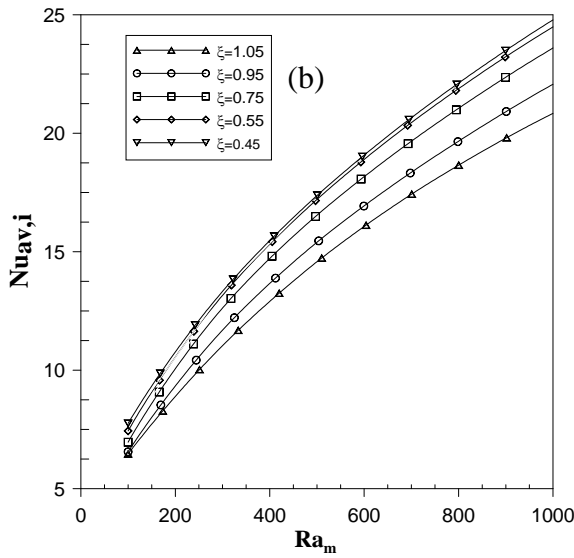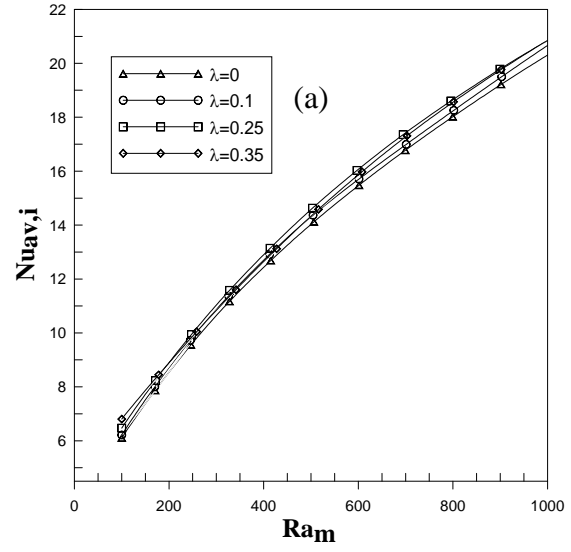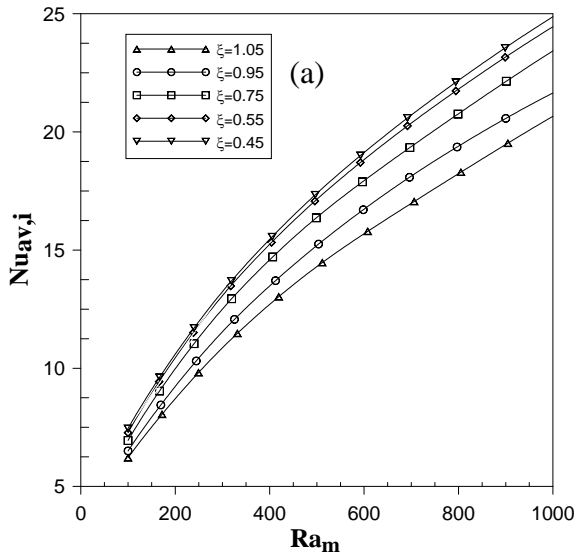Fig.11 Variation of average Nusselt number with Darcy-modified Rayligh Number and ξ for (a) λ=0.1, (b) λ=0.25, (c)λ=0.35

Fig.12 Variation of average Nusselt number with Darcy- modified Rayligh Number and λ for (a) ξ=1.05, (b) ξ=0.7 5, (c) ξ=0.45

APPENDIX 1 (The edited script)

```
TITLE 'WAVY ENCLOSURE HEATED BY INNER CYLINDER'
COORDINATES cartesian2
VARIABLES
Epsi
Theta
 SELECT
 errlim=1e-5
textsize=30
!black=on
paintgrid=off
 DEFINITIONS
 Ra=100   Ar=1.5   a=.25    xc=0  Cy=0.0   yc=Ar/2-Cy        dc= 0.25*Ar
 EQUATIONS
 Epsi:div(grad(Epsi))+Ra*dx(Theta)=0
Theta : dy(Epsi)*dx(theta)-dx(Epsi)*dy(theta)-div(grad(Theta))=0
 BOUNDARIES
 REGION 1
   START(0,0)
Natural (Theta)=0 value(Epsi)=0
 Line to (0.5-a,0)   value(Epsi)=0 value(Theta)=0 line to (0.5-a,0)  #include 'sir.txt'
natural (Theta)=0 value(Epsi)=0 Line to  (a-0.5,Ar)
value(Epsi)=0 value(Theta)=0 line to (a-0.5,Ar)  #include 'sil.txt'
 line to close
 start (xc,yc+dc/2) value(epsi)=0 value(theta)=1arc(center=xc,yc) angle=360
 feature
start 'left side'  (0.5-a,0) line to (0.5-a,0) #include 'sir.txt'
start 'right side'  (a-0.5,Ar) line to (a-0.5,Ar) #include 'sil.txt'
start 'inner rod'  (xc,yc+Dc/2)arc(center=xc,yc)angle=360

PLOTS
 elevation (-normal(grad(Theta))) on 'left side' export format "#d#b#1" file="L.txt"
elevation (-normal(grad(Theta))) on 'right side' export format "#d#b#1" file="R.txt"
 elevation (-normal(grad(Theta)))on 'inner rod' export format "#d#b#1" file="I.txt"
 CONTOUR(Theta)
 CONTOUR(Epsi)
grid(x,y)
 report((line_integral(normal(grad(Theta)),'left side'))) as "AVNUS"
 report((line_integral(-normal(grad(Theta)),'right side'))) as "AVNUS"
 report((line_integral(-normal(grad(Theta)),'inner rod'))) as "AVNUS"
end
```

Note:
sir and sil are text files represent the wavy walls edited from other two separated scripts:

``	```

Title 'Right wall'
 Coordinates cartesian1
 Definitions
Ar=1.5
a = 0.25
 u =(0.5-a)+a*(1-sin ((pi/2)+2*pi*x/Ar))
 Boundaries
 region 1
  start(0)
line (Ar)
 Plots
 elevation(u) from (0) to (Ar) points =5 export format "to (#1,#x)" file="sir.txt"
 end
	Title 'left wall'
	 Coordinates cartesian1
	 Definitions
	Ar=1.50
	a = 0.25
	 u =-(0.5-a)-a*(1-sin ((pi/2)+2*pi*x/Ar))
	 Boundaries
	 region 1
	  start(Ar)
	line (0)
	 Plots
	 elevation(u) from (Ar) to (0) points =5 export format "to (#1,#x)" file="sil.txt"
	 end